LO SVILUPPO DELL'OTTICA QUANTISTICA IN ITALIA

OTTICA QUANTISTICA E INFORMAZIONE QUANTISTICA

Francesco De Martini
Universita' di Roma "La Sapienza

LEOS, Roma, 30 gennaio 2008

GLI ANTESIGNANI*

F. Tito Arecchi, A. Sona CISE Milano (dal 1960)

M.Bertolotti, D. Sette Ist.Bordoni, Roma (dal 1960)

G. Toraldo di Francia Ist. Onde EM, Firenze

Orazio Svelto, E.Gatti Politecnico MI (dal 1963)

- * “Antesignano”: Soldato Romano combattente in prima linea (Devoto-Oli)

INTERNATIONAL SCHOOL E.FERMI (Varenna)

- 1960- Topics of Radiofrequency Spectroscopy
- (dir: A.Gozzini: A. Kastler, A.Javan, A.Abragam, C.H.Townes)
- 1963- Quantum Electronics and Coherent
- Light (dir. C.H.Townes and P.A. Miles)
- 1967- Quantum Optics (dir. R.J.Glauber)
- 1975- Nonlinear Spectroscopy (dir.N.Bloembergen)
- 1991- Laser Manipulation of Atoms and Ions
- (dir. E.Arimondo, W.D.Phillips and F.Strumia)
- 1992- Frontiers in Laser Spectroscopy (T.Hansh, M.Inguscio)
- 2001- Experimental Quantum Computation and
- Information (dir. F. De Martini and C.Monroe)

Proprieta' quantistiche della luce
Photon counting

F.T.Arecchi, E.Gatti, A.Sona, Phys.Lett 16, 1012 (1966)

Quantum Scattering:
Statistical properties in photon-counting and in light-beating Spectroscopy

B.Crosignani, P.Di Porto, M.Bertolotti, "Statistical Properties of Scattered Light" (Academic Press, 1975)

R. Loudon

THE QUANTUM THEORY OF LIGHT

(Oxford 1983)

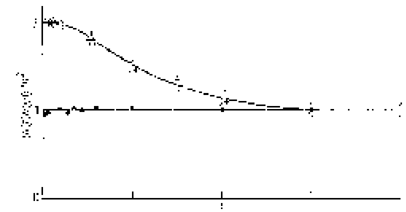

FIG. 6.3. Measured correlations between pairs of photon counts as functions of their time separations for [illegible] and chaotic light of Gaussian frequency distribution (all other points). The [illegible] curves are the same as in Fig. 3.[illegible] (After F. T. Arecchi et al. [illegible])

quantum language of the kind of intensity fluctuations that occur in the classical description of chaotic light, shown in Fig. 3.4. The arrival of a high-intensity fluctuation at the phototube generates closely spaced photon counts, while the arrival of an intensity trough produces very few photon counts. Fig. 6.4(a) shows a schematic representation of the occurrence of photon counts as a function of the time for chaotic light. The clusters of counts, or photon bunches, are clearly visible. Although the extent in time of the bunching is of the order of the coherence time τ_c, we describe light in general as

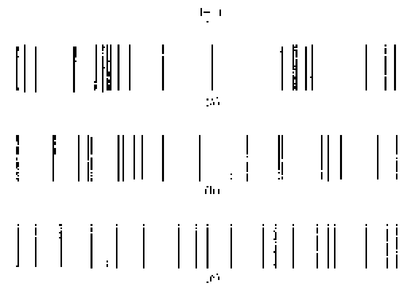

FIG. 6.4. Schematic representations of photon counts as functions of the time for light beams that are (a) bunched with $g^{(2)}(0) > 1$, (b) random with $g^{(2)}(0) = 1$, and (c) antibunched with $g^{(2)}(0) < 1$.

F. T. Arecchi, Eric Courtens
Robert Gilmore, Harry Thomas

“Atomic Coherent States in Quantum Optics”

Phys. Rev. A, 6, 2211 (1972)

Non-linear Spectroscopy

4-photon solid-state Spectroscopy; C.A.R.S. in H2

- J.P.Coffinet and F.De Martini, “Coherent Excitation of polaritons in GaP”, (PRL, 22, 60, 1969)
- F.De Martini, G.P.Giuliani and E.Santamato, “Line profile of the Q(1) vibrational resonance in H2 in the zone of Dicke narrowing” (Opt.Comm. 5, 126, 1972)
- F.De Martini and Y.R.Shen, “Nonlinear excitation of Surface Polaritons” (PRL, 36, 216, 1976)
- F. De Martini, G.Giuliani, P.Mataloni and E.Palange, “Study of Surface Polaritons in GaP by optical 4-wave mixing” (PRL 76, 440, 1976)
- F.De Martini, M.Colocci, S.Kohn and Y.R.Shen, “Nonlinear Optical Excitation of surface exciton Polaritons in ZnO” (PRL, 38, 1223, 1977)
- C.Chen, A.De Castro, Y.R.Shen, F.De Martini, “Surface C.A.R.S.” (PRL, 45, 946, 1979)

4-wave mixing of polaritons in GaP

VOLUME 22, NUMBER 2 PHYSICAL REVIEW LETTERS 13 JANUARY 1969

COHERENT EXCITATION OF POLARITONS IN GALLIUM PHOSPHIDE*

A. Pierre Defrigel and Francesco De Martini
Laboratoire d'Optique Quantique, Institut d'Optique, Faculté des Sciences, Orsay, France
(Received 2[illegible] October 1968)

The coherent excitation of polaritons has been achieved in the III-V semiconductor GaP for the first time by a nonlinear, optical parametric process. We are able to describe the experimental dispersion curve in the [illegible] region and to measure the absorption coefficient of the crystal near the Restrahl band. The results are discussed on the basis of recent theories on the polariton dispersion and damping in GaP.

A high-intensity, coherent polariton field has been excited in the polar III-V semiconductor gallium phosphide by mixing two coherent optical waves whose wavelengths lie in the transmission gap of the crystal. This method for the creation in a medium of coherent, Raman-active (optical) phonons or other elementary excitation is sometimes called "photon-on excitation."

Four pairs of interacting frequencies have been chosen in order to excite resonantly the polarization field near the lattice resonance (Restrahl) at 366 cm^{-1} energy $\hbar\omega_T$ in the lower branch of the optical dispersion curve, a range of infrared wavelengths in which the excitation exhibits a mixed (electromagnetic and phonon) character.[1,2] In our experiment (Fig. 1) two Raman cavities pumped by a Q-switched ruby laser were used to generate two (Stokes) beams of coherent light at different frequencies (ω_1 and ω_2). The two beams were focused by a common high-quality achromatic lens (20-cm $f/1$) on the crystal where the polariton field at frequency $\omega_3 = \omega_1 - \omega_2$ is generated. Small diaphragms were used in front of the lens in order to reduce the convergence of the beams reaching the crystal to about 5×10^{-2}. The angle θ made by the two beams $\vec{k}_1$ and $\vec{k}_2$ in

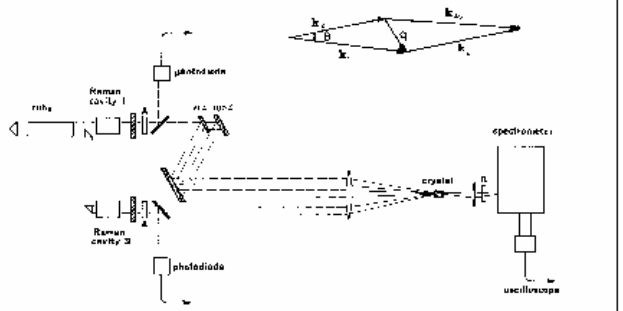

FIG. 1. Schematic diagram of the experimental apparatus.

Effects of photon angular momentum in liquid crystals (LC)

- Spin

  E. Santamato *et al.*, *Collective Rotation of Molecules Driven by the Angular Momentum of Light in a Nematic Film*, Phys. Rev. Lett. **57**, 2423 (1986)

- Orbital

  B. Piccirillo, C. Toscano, F. Vetrano, and E. Santamato, *Orbital and Spin photon angular momentum transfer in liquid crystals,* Phys. Rev. Lett. **86**, 2285 (2001)

Angular momentum in LC

- Liquid crystals are molecular fluids exhibiting both translational and orientational degrees of freedom

  - The photon orbital angular momentum (OAM) *flux* ***L*** induce the rotation of the center of mass of volume element

  - The photon spin angular momentum (OAM) *flux* ***S*** induce changes in the molecular orientation of the volume element

MICROCAVITY and MICROLASER

F. De Martini, G.Innocenti, G.R.Jacobovitz, P.Mataloni, ”Anomalous spon-taneous emission in a Microscopic Optical Cavity” (PRL 59, 2955, 1987)

F. De Martini, G.R.Jacobovitz, “Anomalous Spontaneous-Stimulated decay phase transition and Zero-threshold laser action in a microcavity” (PRL, 60, 1711, 1988)

MICROCAVITY Spontaneous Emission

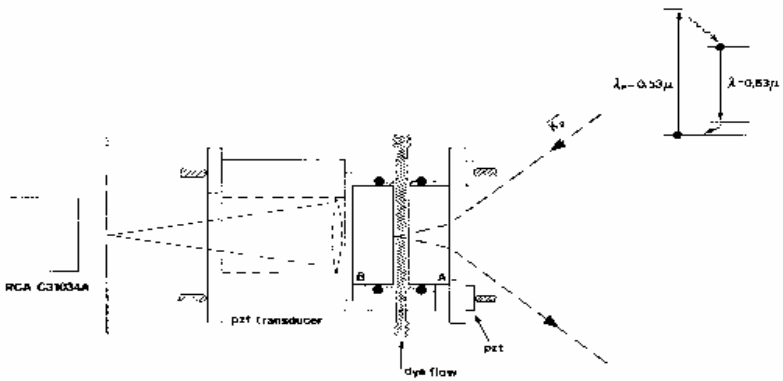

FIG. 1. Microscopic Fabry-Perot cavity (vertical). The directions of the incoming and reflected beams with the excitation wavelength $\lambda_p = 0.53$ μm are shown at the right-hand side.

from mirror B. This last mirror was 96% reflecting for the SE and the pump wavelengths (λ, λ_p), while mirror A was 98%-reflection coated at λ and antireflection coated at λ_p. The SE light emitted from the cavity was filtered by an interference filter centered at $\lambda = 6328$ Å (10-Å pass band), focused on the end of an optical fiber, and then recorded by a large-quantum-efficiency RCA C31034A photomultiplier (2-nsec rise time). The SE waveform data were computer processed by interfacing with a Le-Croy 8013A fast waveform digitizer (1.3-GHz bandwidth). The cavity alignment was maintained by means of two small disk-shaped piezoelectric transducers (PZR) while the cavity spacing was controlled by a Micro-Controle positioner (by 1000-Å steps) and, on a finer scale, by a large cylindrical PZT. We found that, fortunately, the cavity alignment for $d < \lambda$ was kept particularly stable by the surface tension of the dye solution.

The mirror spacing d could be varied over a distance ranging from about 1 mm down to a very small fraction of λ, thus realizing, for $d < \lambda/2$, the remarkable quantum-mechanical effects related to the field-mode elimination and the topological configuration of the Casimir effect [9]. Note that, for $d \simeq \lambda$, the atoms in our cavity were forced to interact resonantly with a single radiation mode, thus realizing, for the first time at optical frequencies, a novel and quite interesting quantum-statistical situation. [7]

In Heisenberg's representation, the dynamics of the single-atom–field coupling is expressed, as usual by a Dicke Hamiltonian written in terms of the time-dependent atomic displacement operators (Π^+, Π) and field operators $(a_k^\dagger, a_k)$ belonging to the modes k.[12] By a Markov approximation, we obtain the evolution equations for the atom and the field belonging to the (single) mode b which is probed out of the cavity, for instance, along the cavity axis:

$$\frac{d}{dt}\langle \Pi^- \Pi \rangle = -\frac{d}{dt}\sum_\nu \langle a_\nu^\dagger a_\nu \rangle \quad (\omega = \omega_\nu), \tag{1a}$$

$$\frac{d}{dt}\langle a_b^\dagger a_c \rangle = -\langle g_c f_b \rangle \langle \Pi^+ \pm_n^N + \text{H.c.} \rangle + \gamma_c \langle \Pi^+ \Pi \rangle. \tag{1b}$$

Equations similar to (1b) may be written for any deexcitation mode k. By solving in first approximation the set of dynamical equations we obtain the (SE) decay rate for an atom placed at a distance z from one of the mirrors and with dipole moment μ orthogonal and parallel to the mirrors, respectively:

$$\Gamma_\perp(z) = A \times 3/(1-R)^2 \times (I_1 - I_2), \tag{2a}$$

$$\Gamma_\parallel(z) = A \times 3/2(1-R)^2 \times (I_1 + I_2), \tag{2b}$$

and

$$I_1(z) = \int_0^{\pi/2} G(\theta, z)\, d\theta,$$

$$I_2(z) = \int_0^{\pi/2} G(\theta, z) \cos^2(\theta)\, d\theta.$$

lead to the expression of the absolute gain at $d=\bar{d}$: $\bar{g}=[2\pi k^2\sqrt{\ln 2}\,|\mu|^2\langle\bar{N}\rangle/2\hbar\omega\Gamma]=G\bar{d}/c$, where μ is the (randomly oriented) transition dipole moment.

For increasing $d>\bar{d}$, i.e., when additional "free" and "cavity-confined" modes become available for atomic deexcitation, the original orderly system at $d=\bar{d}$ becomes a "chaotic" system with rapidly increasing complexity. This leads to the appearance of mode competition and fluorescence loss with reduction of gain and an increase of the threshold-pumping level. The dynamics of the complex system is generally investigated by the methods of nonequilibrium statistical mechanics, i.e., by the Fokker-Planck method[6] and by second-order phase-transition theory.[6,11]

In the context of the latter theory, the behavior of the active microcavity may be understood by analogy with the phenomenologies of ferromagnetism and superconductivity. In our cooperative system the "ordering" process is so overwhelmingly "disorder" (here provided by cavity losses) that, once one photon is stored in the cavity, any additional single SE process provides the symmetry-breaking field to establish a phase transition to the state of nonzero average field $\langle E\rangle$, i.e., to the Glauber coherent-field state, $|\alpha\rangle$.[11] In nonequilibrium laser phase-transition theory the resulting virtual cancellation of the "disorder" phase leads to a zero value of the critical "reservoir variable" which is the "threshold population inversion," $\sigma_t=\langle\bar{\sigma}\rangle_t=0$.[6] From this viewpoint, by analogy with equilibrium problems, our optical system may be thought of as behaving as an *extremely* high-critical-temperature (T_c) ferromagnet or superconductor.[6,11]

In our experiment a piezoelectrically tuned Fabry-Perot microcavity was formed by plane dielectric-coated mirrors, with $f=30$. A flow of sulforhodamine-640 (0.001 ethanol solution, free-space $T=3$ nsec) was kept between the mirrors. The optical pumping of the active medium was provided by second-harmonic generation at $\lambda_p=0.53$ μm by a self-injected Nd-doped yttrium aluminum garnet laser with $\tau=1.5$-nsec pulse duration.[13] The well-collimated laser beam was injected into the cavity through one mirror (A) with a selectable angle θ_p, taken with respect to the cavity axis, z, in order to take advantage of the effect of "periodic optical pumping," a technique allowing us by changes of θ_p to position the pumping zones and then to control the location of the excited molecules in the intracavity space.[1,14] $\theta_p=48°$ was found to correspond to a selective pumping located at $z=\bar{d}/2$ from the mirrors, i.e., in the central transverse section of the cavity. Mirror B, transmitting the detected fluorescence radiation, was 98% reflection coated for λ_p and λ_c, while mirror A was 99% reflection coated at λ_c and antireflection coated at λ_p. The pumping beam had a Gaussian intensity profile with mean diameter $=2$ mm. The fluorescence signal emitted from the cavity was filtered by an ir filter centered at $\lambda=6226$ Å ($\delta=1$ Å passband), focused by a dioptric system with focal length $f=180$ mm on the 4-mm-diam end of an optical fiber, and then recorded by an RCA model C31034A photomultiplier (rise time <1.5 nsec). The cavity alignment was maintained by means of a He-Ne laser through two disk-shaped PZT transducers, while the tuning at $d=\bar{d}$ was controlled by a Micro-Controle positioner by 1000-Å steps and, on a finer scale, by a large toroidal (PZT) transducer. The signal wave forms were recorded with a LeCroy model 8013A fast digitizer while the intensities of the signal and pump beams were recorded through a computer-interfaced analog-to-digital system.

At the SE-enhancement condition, $d=\bar{d}$, the signal pulse width was found to coincide with that of the "pump" pulses at any lowest molecular-excitation level, as expected for StE. The onset of the SE exponential-gain regime (the laser phase transition) taking place at the anomalous threshold pumping intensity, $I_p\propto\sigma_t=0$ for $d=\bar{d}$, is shown in Fig. 1. In Fig. 1, the analogous transition for $d=5\bar{d}$ is reported for comparison. At $d=\bar{d}$ we were not able to determine experimentally a lower limit of the signal intensity for the transition (i.e., we could not find any departure from the exponential law) in spite of the fact that our experimental conditions were not the the idealized ones considered at the beginning of this paper. In fact, a real zero-threshold laser transition should have been found with our technique

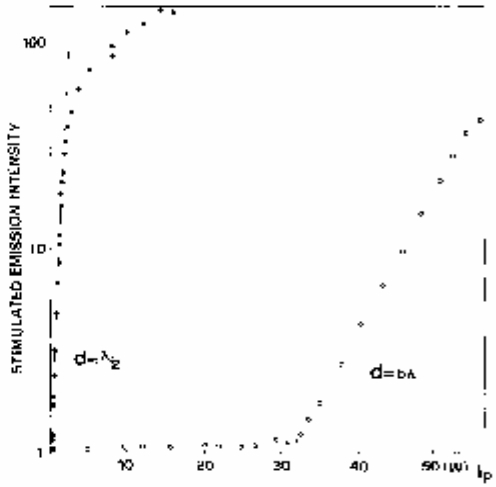

FIG. 1. Laser phase transitions for microcavity dimensions $d=\bar{d}=\lambda/2$ and $d=5\bar{d}$. The emitted intensities shown for $d=5\bar{d}$ should be multiplied by 16 to be compared with the $\bar{d}$ data.

Sub-TW Sub-5-fs Laser Pulses

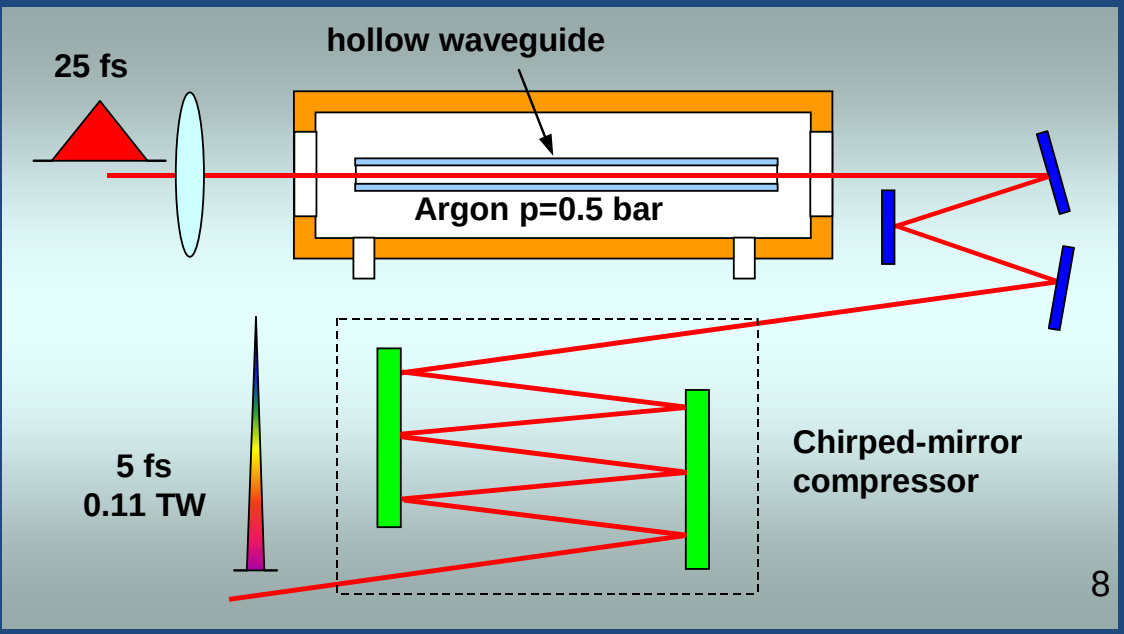

⇒ Ultrabroad-band dispersion control by chirped-mirrors

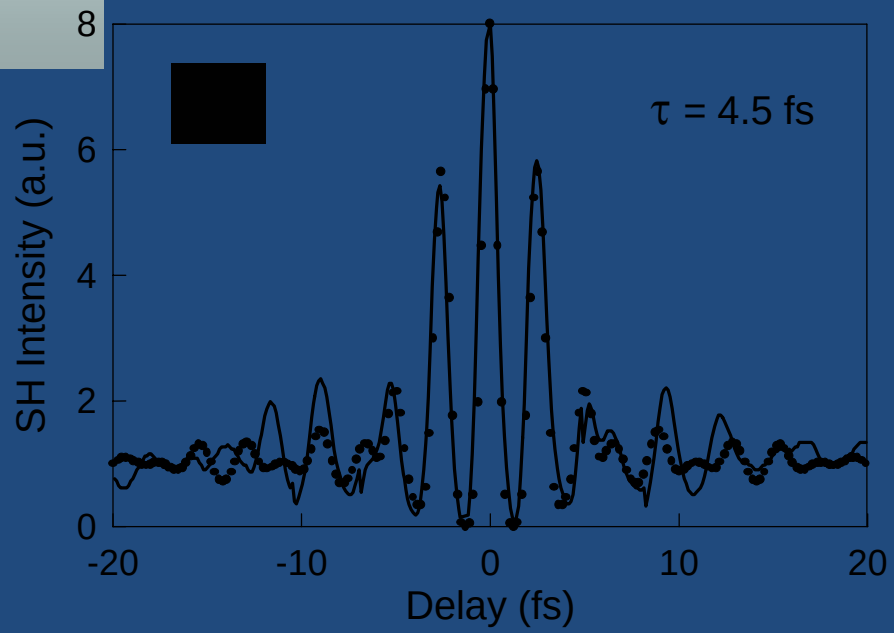

M. Nisoli *et al.*, Appl. Phys. Lett. **68**, 2793 (1996)
M. Nisoli *et al.*, Opt. Lett. **22**, 522 (1997)

Real-time observation of nonlinear coherent phonon dynamics in single-walled carbon nanotubes

A. GAMBETTA[1], C. MANZONI[1], E. MENNA[2], M. MENEGHETTI[2], G. CERULLO[1], G. LANZANI[1]*, S. TRETIAK[3], A. PIRYATINSKI[3], A. SAXENA[3], R. L. MARTIN[3] AND A. R. BISHOP[3]

[1]CNR-INFM, National Laboratory for Ultrafast and Ultraintense Optical Science, Dipartimento di Fisica, Politecnico di Milano, P.za L. da Vinci 32, 20133 Milan, Italy
[2]Department of Chemical Sciences, University of Padova, 1, Via Marzolo, 35131 Padova, Italy
[3]Theoretical Division and Center for Nonlinear Studies, Los Alamos National Laboratory, Los Alamos, New Mexico 87545, USA
*e-mail: guglielmo.lanzani@fisi.polimi.it

Published online: 9 July 2006; doi:10.1038/nphys345

Single-walled carbon nanotubes (SWNTs) are π-conjugated, quasi-one-dimensional structures consisting of rolled-up graphene sheets that, depending on their chirality, behave as semiconductors or metals[1]; owing to their unique properties, they enable groundbreaking applications in mechanics, nanoelectronics and photonics[2,3]. In semiconducting SWNTs, medium-sized excitons (3–5 nm) with large binding energy and oscillator strength are the fundamental excitations[4–6]; exciton wavefunction localization and one-dimensionality give rise to a strong electron–phonon coupling[7–11], the study of which is crucial for the understanding of their electronic and optical properties. Here we report on the use of resonant sub-10-fs visible pulses[12] to generate and detect, in the time domain, coherent phonons in SWNT ensembles. We observe vibrational wavepackets for the radial breathing mode (RBM) and the G mode, and in particular their anharmonic coupling, resulting in a frequency modulation of the G mode by the RBM. Quantum-chemical modelling[13] shows that this effect is due to a corrugation of the SWNT surface on photoexcitation, leading to a coupling between longitudinal and radial vibrations.

Electron–phonon coupling in SWNTs is usually studied using Raman spectroscopy; this technique is useful for investigating ground-state vibrations[14], whereas photoexcited-state vibrational dynamics remain largely unknown because, in the frequency domain, phonon replicas are hardly detectable in the presence of substantial inhomogeneous broadening. Time-domain observation of phonon dynamics has much lower sensitivity with respect to conventional Raman, but it enables direct measurement of excited-state dynamics, vibrational dephasing and mode coupling in a distinct way[15,16]. Coherent phonon detection allows resolution in time of wavepacket dynamics that is otherwise averaged-out in standard Raman scattering.

To detect coherent phonons in SWNTs, we use a standard pump–probe configuration, in which the observed quantity is the modulation depth in the differential transmission[17] ($\Delta T/T$); details of the experimental setup are provided in the Methods section. Figure 1a shows $\Delta T/T$ dynamics of SWNTs grown by the high-pressure carbon monoxide procedure dispersed in polymethylmethacrylate films following excitation with a sub-10-fs visible pulse (1.8–2.4 eV bandwidth), probed at an energy of 2.1 eV. The signal exhibits an initial photobleaching, which quickly turns into photoinduced absorption (PA). The fast photobleaching decay is ascribed to relaxation of the higher-lying exciton (second in an increasing energy scale) to the lower one, taking place with a 40-fs time constant[18]. The PA signal is generated by this lower exciton[4,5] and decays on the ps timescale, in agreement with previous results[19–21]. As shown in Fig. 1a, there is a clear oscillation in the $\Delta T/T$ amplitude. The Fourier transform (FT) of the oscillatory component (Fig. 2a) shows a strong peak at 252 cm^{-1} (132-fs period). This frequency can be recognized as the RBM, associated with expansion and contraction of the tube cross-section[14]. The observation is related to an ensemble of semiconducting SWNTs, with diameters of about 0.95 nm, all vibrating in phase. A similar result is obtained pumping with a 30-fs pulse in the near-infrared (0.92 eV) range and probing in the visible (2 eV) range with a sub-10-fs pulse (Fig. 1b). Here, the lowest exciton is directly excited and its PA rises promptly; a clear modulation at the frequency of 259 cm^{-1} is visible on top of it.

The 'displacive excitation' mechanism[22] can account for coherent phonon generation in SWNTs: carbon atoms do not have time to move during the short pulse excitation. However, in the excited-state electronic configuration, they may have a different equilibrium position. This will occur only for those modes that do not distort the molecular symmetry during vibration, namely totally symmetric modes (those observed in optical transitions and resonance Raman scattering). Calculations based on a semi-empirical excited-state molecular dynamics (ESMD) approach[13] confirm that both the RBM and G modes have substantial coupling with the electronic transitions. Calculated dimensionless displacements from the ground state to the lowest optically active

Coherently Driven Radial Breathing Mode in single wall carbon nanotubes

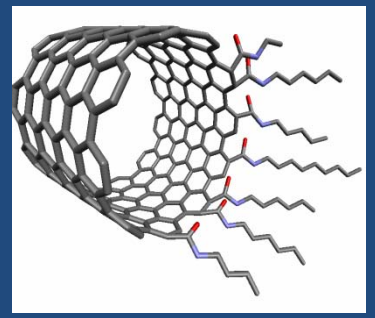

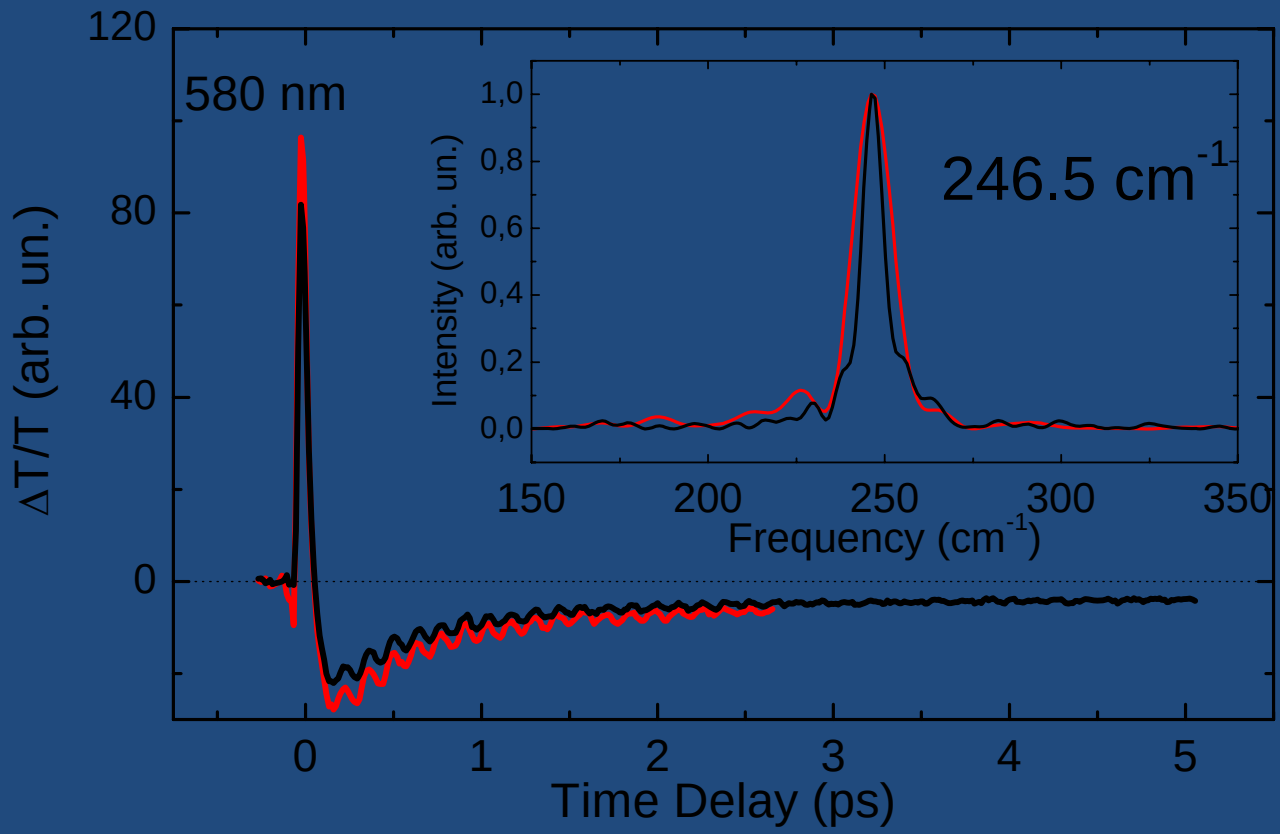

Following the impulsive change in the electronic distribution collective vibrational coherence is initiated in the carbon nanotube ensamble

Entanglement between 2 single photons (EPR, 1935)

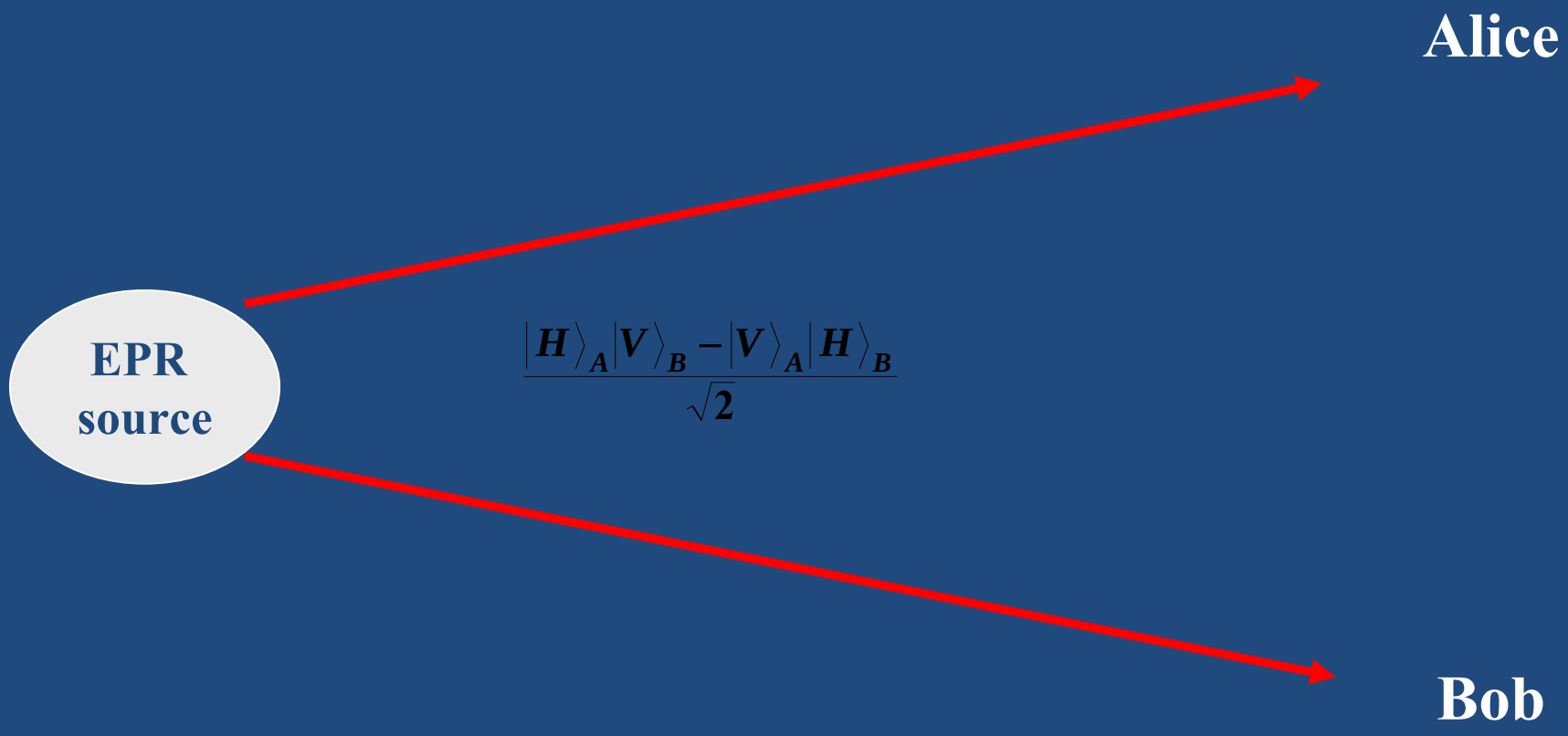

Entanglement between a single photon and a mesoscopic field

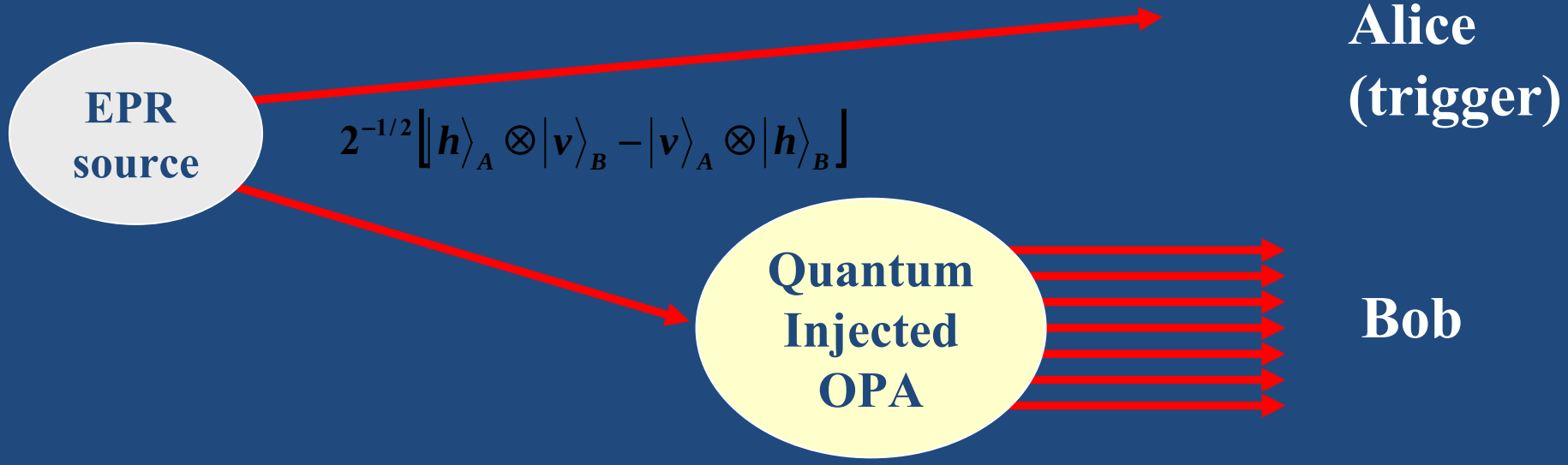

$$|\Sigma\rangle = 2^{-1/2}\left[|h\rangle_A \otimes |\Phi^V\rangle_B - |v\rangle_A \otimes |\Phi^H\rangle_B\right]:$$

SCHROEDINGER CAT STATE

From the microscopic to the macroscopic world

Entanglement: “the characteristic trait of Quantum Mechanics” (Schrödinger)

$$2^{-1/2}\left(|H\rangle_A|V\rangle_B - |V\rangle_A|H\rangle_B\right)$$

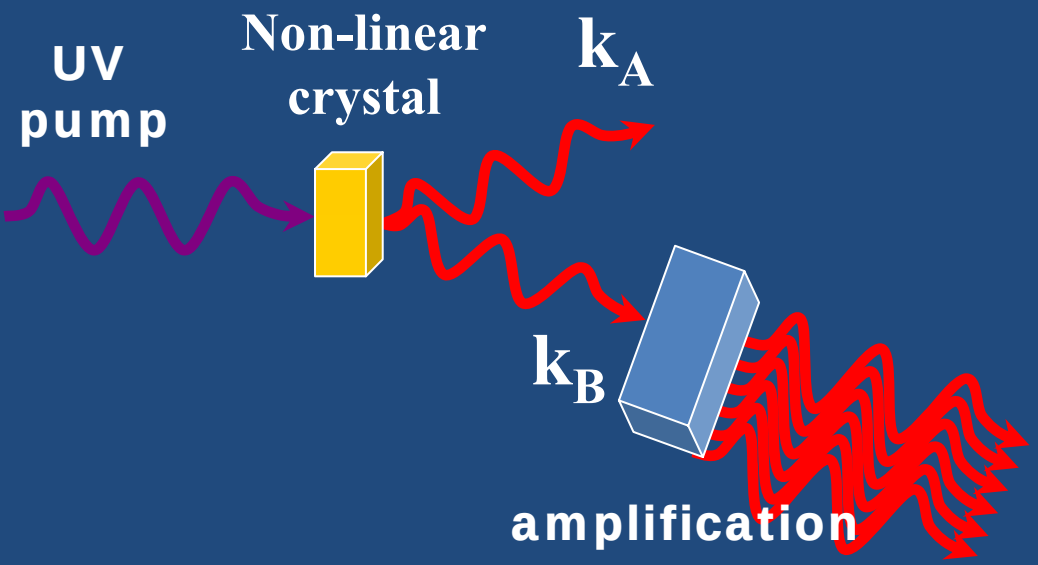

Macroscopic Optical Parametric Amplifier

Injection: Quantum state (single photon state)

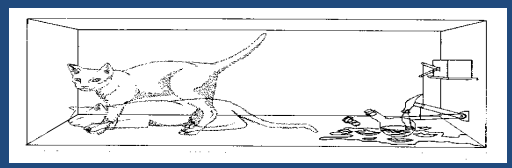

$$|\Sigma\rangle = \frac{1}{\sqrt{2}}\left(|H\rangle \right.$$  $$\left. + |V\rangle \right.$$  $$\left.\rangle\right)$$

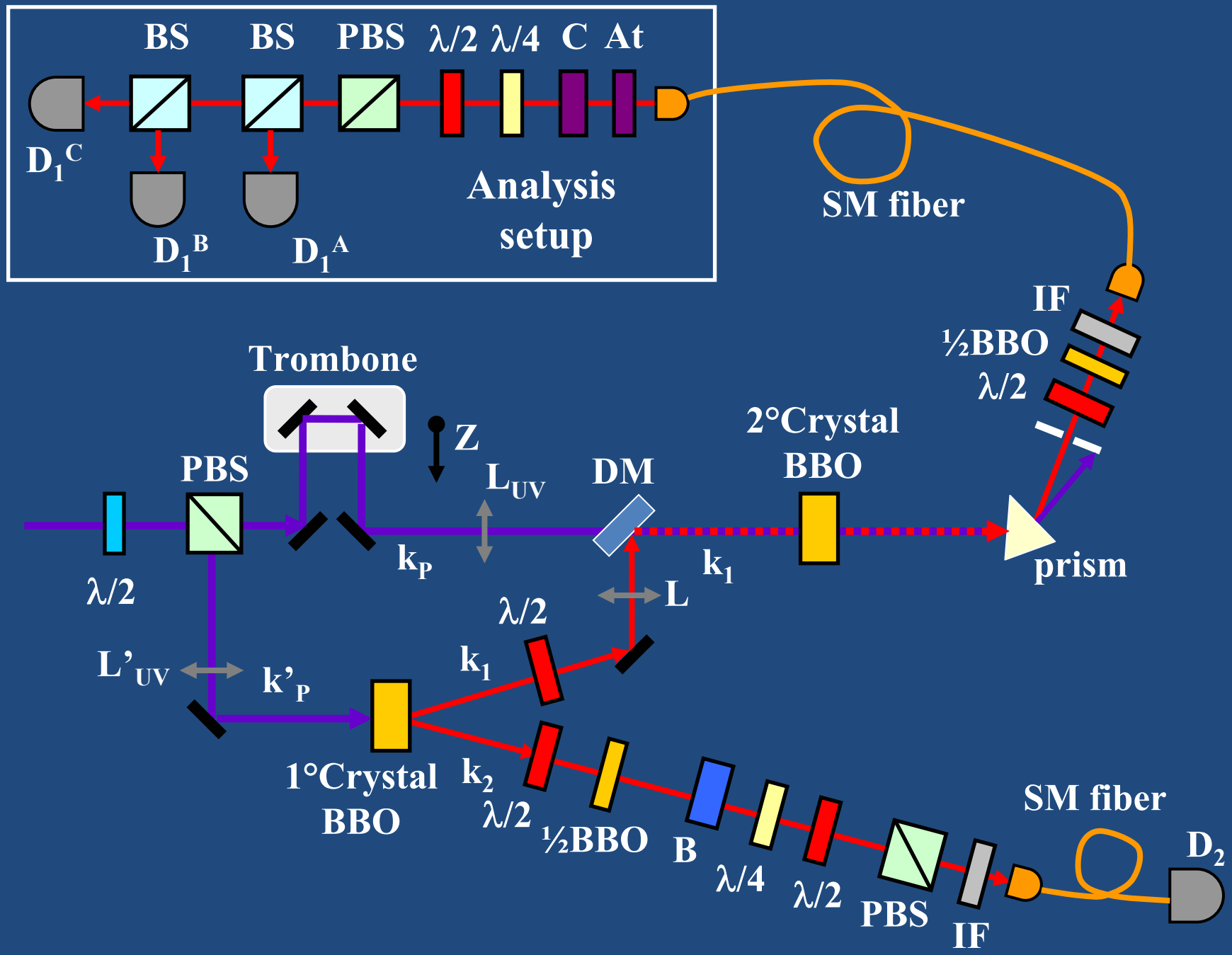
BS
BS
PBS
λ/2
λ/4
C
At
D_1^C
D_1^B
D_1^A
Analysis setup
SM fiber
IF
½BBO
λ/2
Trombone
Z
PBS
L_{UV}
DM
2°Crystal BBO
prism
λ/2
k_P
k_1
L
λ/2
L'_{UV}
k'_P
k_1
1°Crystal BBO
k_2
λ/2
½BBO
B
λ/4
λ/2
PBS
IF
SM fiber
D_2

COLLECTIVE MACROSCOPIC ATOMIC DISPLACEMENT

by coherent Bragg scattering with photon-atom momentum exchange:

QI-OPA MIRROR-BEC

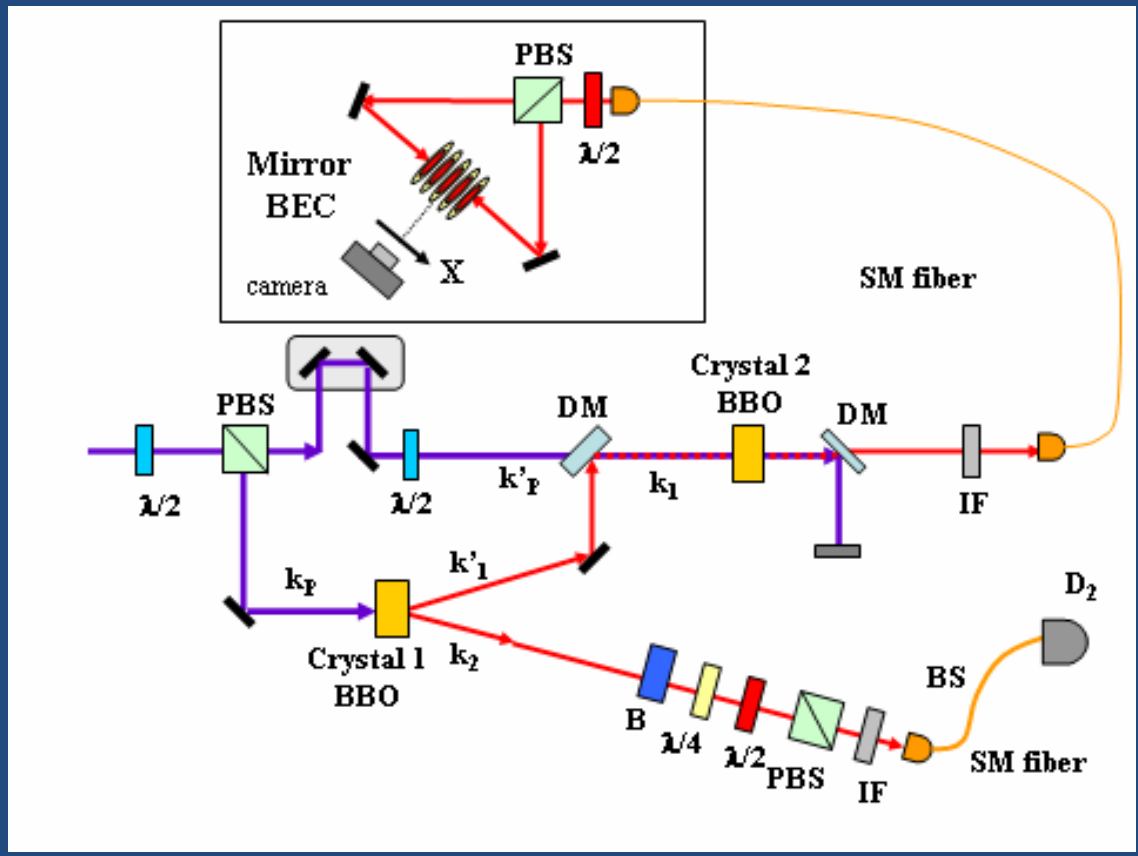
PBS
λ/2
Mirror
BEC
camera
X
SM fiber
PBS
DM
Crystal 2
BBO
DM
λ/2
λ/2
k'P
k1
IF
k'1
kP
D2
Crystal 1
BBO
k2
BS
B
λ/4
λ/2
PBS
IF
SM fiber

QI-OPA DRIVEN BEC MECHANICAL OSCILLATIONS

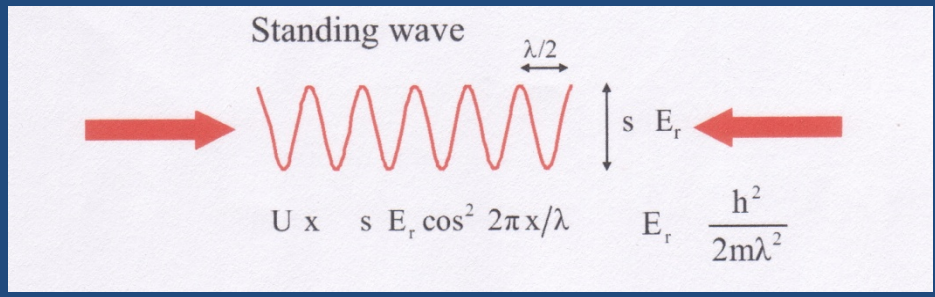

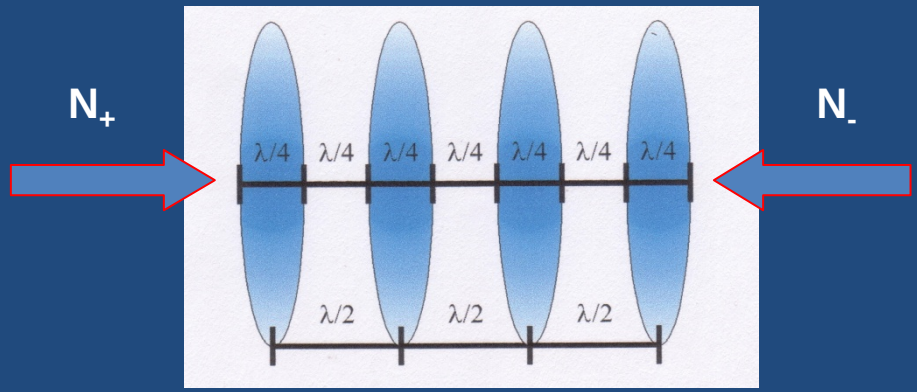

SUPERRADIANT RAYLEIGH SCATTERING → BRAGG SCATTERING:
L.De Sarlo et al (LENS Group) Eur.Phys. J.D. (2004)
L.Fallani et al. (LENS Group) PRA 71, 033612 (2005)

Condensate in a Lattice

The ground state consists of an array of disk shaped condensates each residing in a node of the optical standing wave while tunnelling through the optical barriers keeps phase coherence through the array

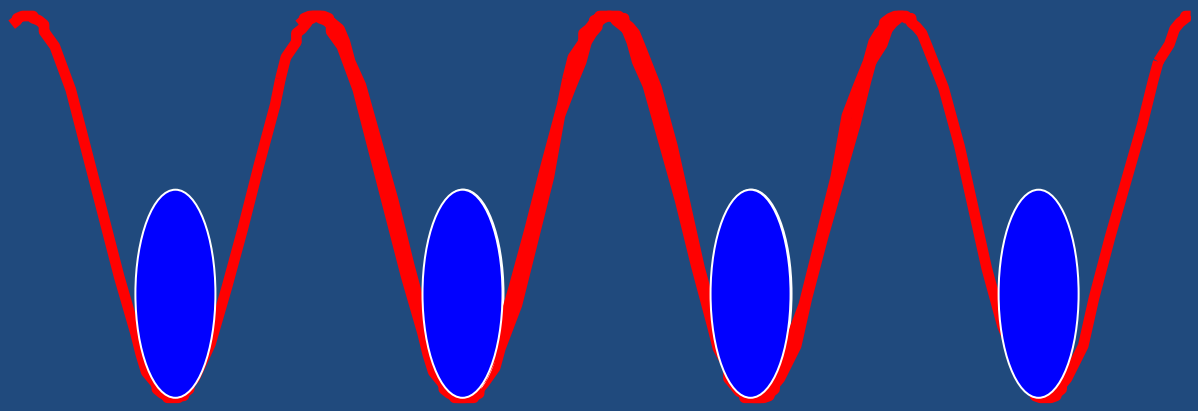

Entanglement between 2 mesoscopic fields (de-coherence free) [Near future]

$$\frac{|H\rangle_A|V\rangle_B - |V\rangle_A|H\rangle_B}{\sqrt{2}}$$

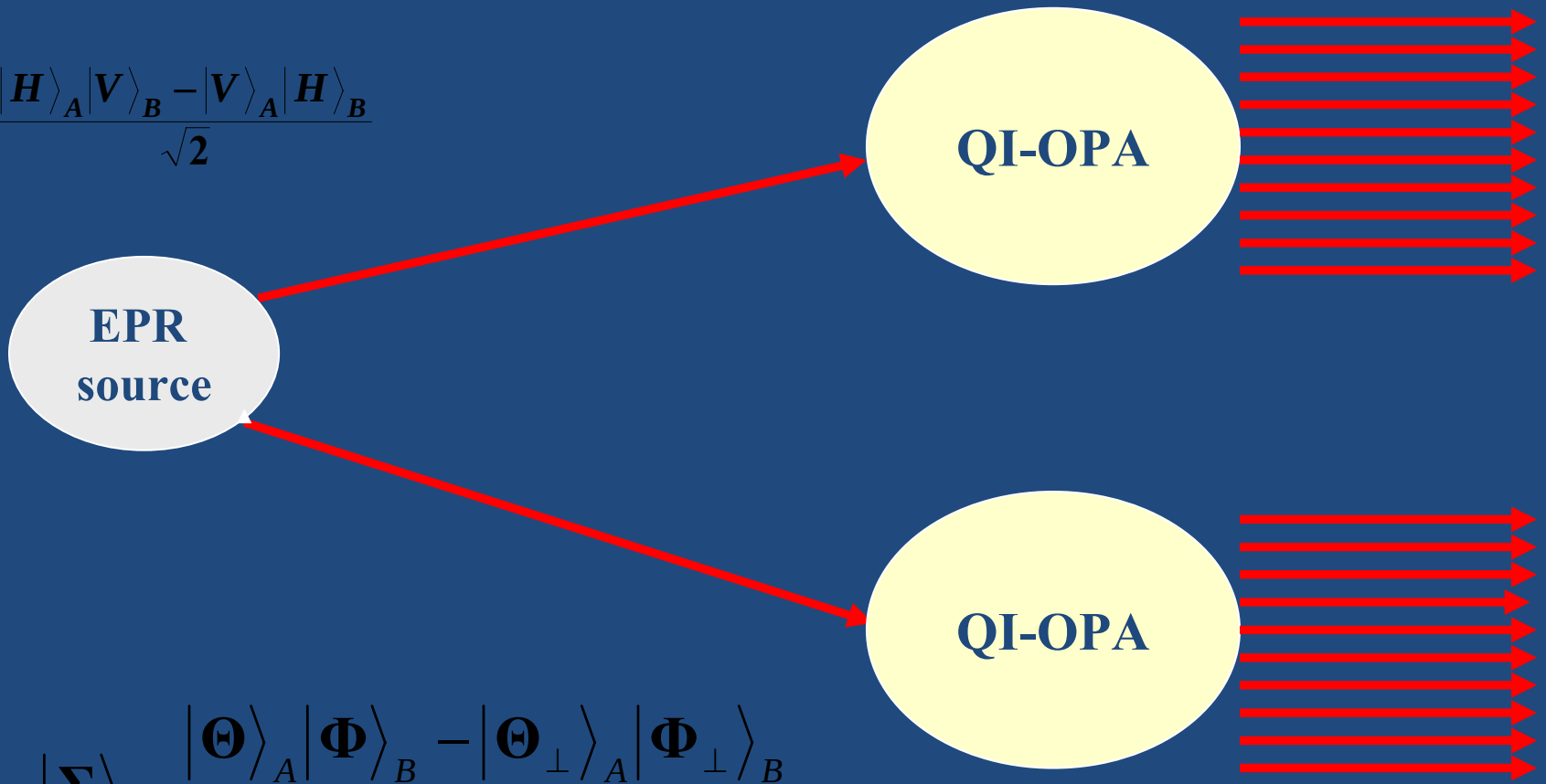

$$|\Sigma\rangle = \frac{|\Theta\rangle_A|\Phi\rangle_B - |\Theta_\perp\rangle_A|\Phi_\perp\rangle_B}{\sqrt{2}}$$